Turbulent viscosity in natural surf zones

F. Grasso[1,2] and B. G. Ruessink[1]

Received 5 October 2012; revised 31 October 2012; accepted 31 October 2012; published 4 December 2012.

[1] Waves breaking in the shallow surf zone near the shoreline inject turbulence into the water column that may reach the bed to suspend sediment. Breaking-wave turbulence in the surf zone is, however, poorly understood, which is one of the reasons why many process-based coastal-evolution models predict coastal change during severe storms inadequately. Here, we use data collected in two natural surf zones to derive a new parameterization for the stability function C_μ that determines the magnitude of the eddy viscosity ν_t in two-equation turbulent-viscosity models, $\nu_t = C_\mu k^2/\varepsilon$, where k is turbulent kinetic energy and ε is the turbulence dissipation rate. In both data sets, the ratio of turbulence production to dissipation is small (≈0.15), while vertical turbulence diffusion is significant. This differs from assumptions underlying existing C_μ parameterizations, which we show to severely overpredict observed C_μ for most conditions. Additionally, we rewrite our new C_μ parameterization into a formulation that accurately reproduces our Reynolds-stress based estimates of turbulence production. This formulation is linear with strain, consistent with earlier theoritical work for large strain rates. Also, it does not depend on ε and can, therefore, also be applied in one-equation turbulent-viscosity models. We anticipate our work to improve turbulence modeling in natural surf zones and to eventually lead to more reliable predictions of coastal evolution in response to severe storms. **Citation:** Grasso, F., and B. G. Ruessink (2012), Turbulent viscosity in natural surf zones, *Geophys. Res. Lett.*, *39*, L23603, doi:10.1029/2012GL054135.

1. Introduction

[2] Storm waves often erode sandy beaches and dunes, endangering human life, and ecologic and economic resources; however, current coastal-evoluation models are not able to accurately predict coastal change during high-energy breaking-wave conditions [e.g., *Ruessink and Kuriyama*, 2008]. An important reason may be the hitherto poorly understood vertical structure of turbulence under breaking waves [e.g., *Feddersen*, 2012b] and their effect on sand suspension and transport [e.g., *Scott et al.*, 2009].

[3] Turbulence models, such as the widely adopted $k-\varepsilon$ model [*Rodi*, 1987], where k is the turbulent kinetic energy and ε the turbulent dissipation rate, need closure equations to model the turbulence and to resolve the momentum equations and the mass conservation in the water column. The concept of turbulent (eddy) viscosity, ν_t, is an important aspect in closure models to express turbulence production and diffusion in terms of k, ε and mean flow parameters [e.g., *Mellor and Yamada*, 1982]. In the sea-bed boundary layer under non-breaking waves, the turbulence equations are often written as a balance between shear production and dissipation [e.g., *Tennekes and Lumley*, 1972; *Trowbridge and Elgar*, 2001], assuming turbulence diffusion to be negligible. Turbulence production P can be formulated as $P = \nu_t S^2$, where S^2 is the squared shear frequency and $\nu_t = C_\mu k^2/\varepsilon$ [e.g., *Pope*, 2000]. The stability function C_μ results from algebraic second-moment turbulence closures. In the $k-\varepsilon$ model C_μ is set to the constant value of 0.09 to give the correct turbulent shear stress in plane thin shear flows ($P \approx \varepsilon$). The few existing field studies on turbulence beneath breaking waves [e.g., *Feddersen*, 2012a] indicate that production does not balance dissipation anymore. Furthermore, laboratory experiments showed that diffusion of turbulence, especially the vertical turbulent transport, can play a significant role in turbulence dynamics [e.g., *Ting and Kirby*, 1996; *Melville et al.*, 2002]. These nonequilibrium conditions between P and ε lead to a nonlinear behavior of C_μ. How to estimate C_μ, and hence ν_t, is one of the main concerns in $k-\varepsilon$ model development and is the focus of the present paper.

[4] Recent progress in the modeling of nonlinear stability functions was based on the development of explicit algebraic models (EAMs), especially in the field of oceanography [e.g., *Wallin and Johansson*, 2000; *Canuto et al.*, 2001; *Umlauf and Burchard*, 2005; *Violeau*, 2009]. Using the weak-equilibrium assumption [*Pope*, 1975; *Rodi*, 1976], EAMs were developed to meet increasing demands for the prediction of complex flows. As demonstrated by *Burchard and Bolding* [2001], the second-moment closure model of *Canuto et al.* [2001] was superior to other models in terms of physical soundness, predictability, computational economy, and numerical robustness. *Canuto et al.*'s [2001] stability function, $C_{\mu C01}$, depends on the nondimensional shear number $\alpha_M = S^2k^2/\varepsilon^2$,

$$C_{\mu\,C01} = (0.107 - 0.00012\alpha_M)/\left(1 + 0.02872\alpha_M - 0.0000337\alpha_M^2\right). \quad (1)$$

This equation is commonly used to model the ocean boundary layer under wave breaking in deep water (≈100–200 m) [e.g., *Burchard*, 2001; *He and Chen*, 2011]; its only application to a nearshore setting in ≈4.5 m depth [*Feddersen and Trowbridge*, 2005] resulted in a clear overestimation of ν_t, albeit that the data-model comparison was restricted to a single-point above

[1]Department of Physical Geography, Faculty of Geosciences, Institute for Marine and Atmospheric Research, Utrecht University, Utrecht, Netherlands.
[2]Now at Laboratoire DYNECO-PHYSED, IFREMER, Plouzané, France.

Corresponding author: F. Grasso, Laboratoire DYNECO-PHYSED, IFREMER, BP70, FR-29280 Plouzané CEDEX, France. (florent.grasso@ifremer.fr)

0094-8276/12/2012GL054135

the bed. Following *Wallin and Johansson* [2000], combining their equations (2.2) and (2.3), C_μ can also be formulated as a function of P/ε,

$$C_{\mu\,\mathrm{WJ00}} = 6/[10(c_1' + 2.25P/\epsilon)], \quad (2)$$

with $c_1' = 2.25(c_1 - 1)$ and $c_1 = 1.8$. Because $P/\varepsilon = \alpha_M C_\mu$, $C_{\mu\,\mathrm{WJ00}}$ is, as $C_{\mu\,\mathrm{C01}}$, a function of α_M. In regions of the flow where P/ε is small, the assumption of negligible effects of advection and diffusion may cause C_μ to be too large, leading to an overestimation of the Reynolds stress and, hence, the shear production [see also *Taulbee*, 1992].

[5] Here, we explore the behavior of C_μ beneath depth-limited, shallow-water breaking waves from two field data set complimentary in wave and current characteristics. Consistent with equations (1) and (2), we find observed C_μ to depend on α_M. Because observed and predicted C_μ do not agree in an absolute sense, we propose a new C_μ parameterization, which results in a P formulation that varies linearly with S and does not depend on ε. We expect our C_μ and P formulations to improve turbulence modeling in natural surf zones and to eventually lead to more reliable predictions of coastal evolution in response to severe storms.

2. Data and Methods

2.1. Data Collection

[6] We use data from two recent field experiments. The first data set was collected at Truc Vert beach on the French Atlantic coast [*Ruessink*, 2010; *Sénéchal et al.*, 2011; *Grasso et al.*, 2012]. An instrumented rig was positioned on an ≈1:40 plane section of the N-S oriented intertidal beach (median grainsize D_{50} = 400 μm), and was constructed to minimize flow disturbance for cross-shore propagating waves and southward alongshore currents. The rig was equipped with three single-point, sideways oriented, SonTek acoustic Doppler velocimeter ocean (ADVO) probes stacked in a 0.43 m high vertical array with equal distance between ADVO1, 2, and 3 (ADVO number increases upward), all sampling at 10 Hz in one burst of 1460 s each half hour. Each ADVO had a build-in pressure sensor. The second data set was obtained on the 1:70 sloping, E-W oriented, intertidal beach of Ameland, the Netherlands [*Ruessink et al.*, 2012], with $D_{50} \approx 200$ μm. Now, the ADVOs were downward oriented with the probes stacked in a 0.45 m high vertical array, where the vertical distance between ADV01 and ADVO2 was 0.15 m, and that between ADVO2 and ADVO3 0.30 m. At Ameland, measurements were conducted in bursts of 1740 s each half hour with a sampling frequency of 10 Hz. The ADVO and pressure data during both deployments were processed and quality controlled using a previously used procedure [*Ruessink*, 2010]. Positive cross-shore u, alongshore v, and vertical w velocity were onshore, southward and eastward at Truc Vert and Ameland, respectively, and upward directed.

[7] Here we focus on a 12-day period from 7 to 19 March 2008 for the Truc Vert experiment, and on a 4-day period from 23 to 27 September 2010 for the Ameland experiment, when all 3 sensors worked well and bed level was accurately known. During these periods, the offshore (in ≈200 m water depth) significant wave height H_{s0} ranged between 2–8 m (0.5–3.5 m) at Truc Vert (Ameland), with significant periods between 6–14 s (4–8 s). At the rig, the sea-swell (0.04–1 Hz) H_s ranged between 0.5–2 m (0.5–1 m) and the water depth h between 1–3.5 m (1–2 m). The local H_s were depth-modulated, representative of a depth-limited surf zone; the relative wave height H_s/h, which can be used as a proxy of breaking intensity [e.g., *Ruessink*, 1998], varied between 0.4–0.6 (0.4–0.55). Waves were observed to break by both plunging and spilling, and were mostly shore-normally incident due to refraction over the seaward morphology. The burst-averaged cross-shore $\overline{u}$ and alongshore $\overline{v}$ velocities reached maximum values of −0.43 (−0.23) and −1.13 m/s (±0.48 m/s), respectively. The ADVO elevations above the bed, z, ranged between 0.16–1.18 m (0.3–0.82 m). Except during the most energetic conditions, bed forms at the Truc Vert rig were ubiquitous [*Ruessink*, 2010; *Sénéchal et al.*, 2011], including wave-driven vortex ripples (height $\eta \approx 0.15$ m, length $\lambda \approx 0.5$ m) and 0.4 m deep pits related to megaripples. In contrast, in the Ameland data set, the sea bed was essentially flat throughout the selected period.

2.2. Methodology

[8] From our observations, we estimated C_μ as

$$C_{\mu\,\mathrm{exp}} = P_{Re}\varepsilon/\left(S^2k^2\right), \quad (3)$$

where $P_{Re} = \left[-\overline{u'w'}\partial_z\overline{u} - \overline{v'w'}\partial_z\overline{v}\right]$, $S^2 = \left[(\partial_z\overline{u})^2 + (\partial_z\overline{v})^2\right]$, and $k = 0.5\left[\overline{(u')^2} + \overline{(v')^2} + \overline{(w')^2}\right]$. For ADVO1, P_{Re} and S were based on vertical gradients between ADVO1 and 2; for ADVO2, between ADVO1 and 3; and for ADVO3, between ADVO2 and ADVO3. The turbulence fluctuations u', v', and w', and hence k and the shear (Reynolds) stresses $\overline{u'w'}$ and $\overline{v'w'}$, were estimated using the two-sensor differencing-filtering technique of *Feddersen and Williams* [2007]. Turbulence estimates at ADVO1 used adaptive-filtered velocities from ADVO3, whereas ADVO2 and ADVO3 used adaptive-filtered velocities from ADVO1. Following heuristic guidelines in *Feddersen and Williams* [2007], we discarded u', v', and w' estimates when the co-spectra of $\overline{u'w'}$ and $\overline{v'w'}$ showed considerable wave bias [see also *Ruessink*, 2010]. Many bursts did not pass this quality control, especially at ADVO3. From the initial 577 (193) bursts collected at Truc Vert (Ameland), we retained $n_{TV1} = 25$, $n_{TV2} = 57$, $n_{TV3} = 12$ ($n_{A1} = 18$, $n_{A2} = 47$, $n_{A3} = 27$) good data bursts at ADVO1, 2 and 3, respectively. Because u', v', and w' can be biased high by instrument noise [e.g., *Hurther and Lemmin*, 2001; *Scott et al.*, 2005], the magnitude of the Doppler noise variance was estimated from the high-frequency (3–5 Hz) portion of the u, v and w spectra. In the estimation of k, these noise variances were subtracted from the cross-shore, alongshore, and vertical turbulence variances, which reduced k by ≈10–15%. For each burst that passed the wave-bias quality control, ε was estimated [*Gerbi et al.*, 2009] from the 1.5–3 Hz [*Ruessink*, 2010] frequency range in the cross-shore velocity spectra for Truc Vert and from the vertical velocity spectra for Ameland. All ε estimates passed the quality control measures proposed by *Feddersen* [2010]. We note that in the application of equation (3), k and ε were taken as the mean of the values at ADVO1 and 2, and at ADVO2 and 3,

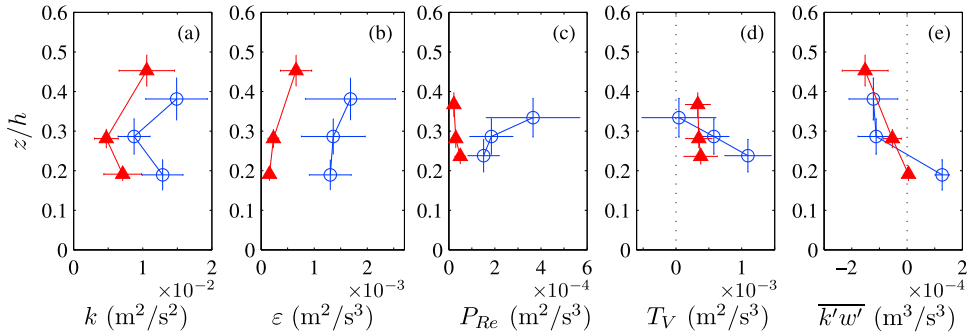

Figure 1. Vertical structures of (a) turbulent kinetic energy k, (b) turbulent dissipation rate ε, (c) Reynolds-stress turbulent production P_{Re}, (d) vertical turbulent transport T_V, and (e) vertical turbulent fluxes $\overline{k'w'}$. Profiles represent the mean values at ADVO1, 2 and 3 with regard to the relative position in the water column z/h ($z/h = 0$ at the sea bed, $z/h = 1$ at the sea surface, and the wave-trough level is at $z/h \approx 0.7$). To have coherent vertical structures, only simultaneous good data bursts at the three ADVOs were selected, leading to $n_{TV} = 10$ and $n_A = 8$ profiles for Truc Vert (open circles) and Ameland (solid triangles) experiments, respectively. As P_{Re} and T_V were based on vertical gradients, the three vertical estimates were computed between ADV0 1–2, 1–3 and 2–3, explaining the different relative position z/h in Figures 1c and 1d compared to Figures 1a, 1b, and 1e. Vertical and horizontal brackets represent 95% confidence intervals.

respectively, to yield $C_{\mu\,\mathrm{exp}}$ estimates at the same vertical location as for the gradient estimates in P, P_{Re}, and S.

3. Results and Discussion

[9] Before we compare $C_{\mu\,\mathrm{exp}}$ to C_μ estimates using equations (1) and (2), we first examine the vertical structure of k, ε, P_{Re}, the vertical turbulence flux $\overline{k'w'}$, and its vertical gradient, the vertical turbulent transport $T_V = \partial_z \overline{k'w'}$ (Figure 1). Here, k' refers to the instantaneous turbulent kinetic energy. T_V provides an estimate of turbulent diffusion D, $D = T_V + P_V + D_v$; we cannot estimate the pressure turbulent transport P_V from our data and the molecular diffusion D_v is negligible for high Reynolds numbers. As can be seen in Figure 1a, the vertical structure of k was similar for both experiments, with k increasing to the sea bed and to the sea surface. This signifies the importance of both bed-generated and breaking-induced, surface-injected turbulence. The magnitude of k was much lower in the Ameland data, $k_A \approx 0.55\ k_{TV}$. This difference in magnitude is even more pronounced for ε ($\varepsilon_A \approx 0.15\varepsilon_{TV}$), with again the vertical structure about the same. The vertical structure of P_{Re} differed markedly in both data sets, with P_{Re} increasing toward the sea surface at Truc Vert and to the sea bed at Ameland, respectively (Figure 1c). In the Truc Vert data the production was mainly generated by shear in the cross-shore mean flow ($P_u \approx 2.6\ P_v$, with P_u and P_v the cross-shore and alongshore components of production, respectively), even though $|\overline{v}|$ reached 1 m/s; in contrast, the production in the Ameland data was mainly alongshore generated ($P_u \approx 2.1\ P_v$). Why the two data sets differ in this way is not fully understood; it might be related to the different bed form characteristics or horizontal flow patterns (the bathymetry at Truc Vert was strongly alongshore variable [*Almar et al.*, 2010] with associated meandering and rip-current flows [*MacMahan et al.*, 2010]; the local Ameland bathymetry was much more uniform). It can easily be deduced from Figures 1b and 1c that P_{Re} did not balance ε, $P_{Re} \approx 0.14\varepsilon$, in both data sets. Intriguingly, estimates of vertical turbulent transport were substantial in both data sets (Figure 1d), on average even larger than the production. Positive T_V corresponds to a source of turbulence balancing turbulence dissipation. Consequently, we clearly see that diffusion was a significant actor in the turbulence dynamics in our shallow-water surf zones. Looking at the vertical turbulent fluxes in Figure 1e, negative $\overline{k'w'}$ at ADVO2 and3 represent downward fluxes induced by wave-breaking turbulence at the sea surface, whereas positive $\overline{k'w'}$ at ADVO1 represent upward fluxes induced by bed-boundary-layer turbulence at the sea bed. Note that $\overline{k'w'}$ was larger at Truc Vert's ADVO1, potentially related to large bed forms present at Truc Vert.

[10] Figure 2 shows $C_{\mu\,\mathrm{exp}}$ versus $\alpha_{M\,\mathrm{exp}}$, together with $C_\mu = 0.09$ and the C_μ estimated from equations (1) and (2). $C_{\mu\,\mathrm{WJ00}}$ has to be estimated iteratively; we started with an initial value of 0.09 and found $C_{\mu\,\mathrm{WJ00}}$ to change less than 1% within 30 iterations. It is obvious from Figure 2 that all three approaches overestimated the experimental results for almost the entire $\alpha_{M\,\mathrm{exp}}$ range, likely caused by the assumed negligible importance of turbulence diffusion [*Taulbee*,

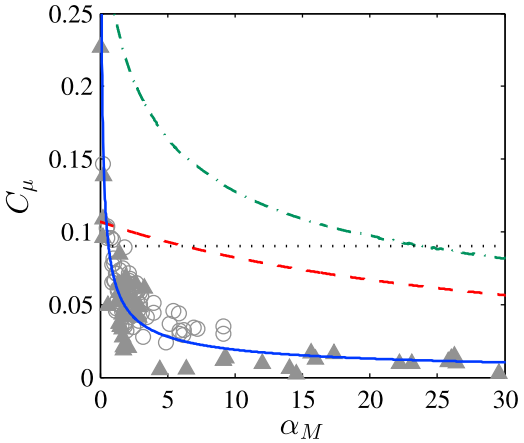

Figure 2. Stability function C_μ versus nondimensional shear number α_M for Truc Vert (open circles) and Ameland (solid triangles) experiments, $C_\mu = 0.09$ (dotted), $C_{\mu\,\mathrm{WJ00}}$ (dash-dotted), $C_{\mu\,\mathrm{C01}}$ (dashed), and the empirical formula derived from the experiments $C_{\mu\,\mathrm{emp}}$ (solid).

Table 1. Coefficients a and b With 95% Confidence Interval in the Best-Fit $C_{\mu\ \mathrm{emp}} = a\alpha_M^b$, Correlation Coefficient Squared r^2 and Root-Mean-Square Error e_{rms} Between $C_{\mu\ \mathrm{emp}}$ and $C_{\mu\ \mathrm{exp}}$

	Truc Vert	Ameland	Truc Vert + Ameland
a	0.071 ± 0.005	0.050 ± 0.011	0.069 ± 0.006
b	-0.40 ± 0.07	-0.54 ± 0.10	-0.56 ± 0.06
r^2	0.69	0.80	0.65
e_{rms}	0.011	0.026	0.031

1992; *Wallin and Johansson*, 2000] and contrasting with our observations (Figure 1). Intriguingly, $C_{\mu\ \mathrm{WJ00}}$ followed the same tendency as the observations. In absolute sense, $C_{\mu\ \mathrm{C01}}$ agreed best with the observations, especially at $\alpha_{M\ \mathrm{exp}} < 2$; for larger $\alpha_{M\ \mathrm{exp}}$, $C_{\mu\ \mathrm{C01}}$ overestimated $C_{\mu\ \mathrm{exp}}$ by a factor of 3 to 5. This is consistent with *Feddersen and Trowbridge*'s [2005] observation that $C_{\mu\ \mathrm{C01}}$ leads to an overestimated ν_t. The dependence of $C_{\mu\ \mathrm{exp}}$ on α_M in both data sets is similar and suggests a parameterization in the form of $C_{\mu\ \mathrm{emp}} = a\alpha_M^b$, with a and b empirical coefficients. A least-square fit with the data from the two data sets combined results in,

$$C_\mu = 0.069\alpha_M^{-0.56}, \tag{4}$$

with a 95% confidence range of 0.012 for a and of 0.12 for b, see Figure 2. The correlation coefficient squared r^2 of the fit amounted to 0.65 and the root-mean-square difference e_{rms} between $C_{\mu\ \mathrm{exp}}$ and the fit (4) to 0.031. Values for a, b, r^2 and e_{rms} for the Truc Vert and Ameland data sets independently are similar (Table 1), which is reassuring given the different turbulence dynamics deduced from Figure 1.

[11] Uncertainties in our turbulence estimates may effect $C_{\mu\ \mathrm{exp}}$, and hence the coefficients in equation (4). Based on laboratory experiments with regular waves and with repeated sets of random waves, *Scott et al.* [2005] demonstrated that the differencing method might bias high k by some 26%, when compared to results from a potentially more accurate ensemble-averaging technique [*Svendsen*, 1987]. If we lower our k as $k_{\mathrm{cor}} = \gamma k$, with $\gamma = 1/1.26$ and consider the same correction for the variance of the turbulent velocities, then $C_{\mu\ \mathrm{exp}} = \left(-\overline{u'w'}\partial_z\overline{u} - \overline{v'w'}\partial_z\overline{v}\right)\varepsilon/(S^2k^2)$ would change by a factor γ/γ^2, as $C_{\mu\ \mathrm{cor}} = 1/\gamma C_{\mu_2\mathrm{exp}}$. Similarly, $\alpha_M = S^2k^2/\varepsilon^2$ would change into $\alpha_{M\ \mathrm{cor}} = \gamma^2\alpha_M$. This would lead to $C_{\mu\ \mathrm{emp,cor}} = a_c\alpha_M^{b_c}$ with best-fit values $a_c = 0.067 \pm 0.005$ and $b_c = -0.56 \pm 0.06$. These coefficients are almost identical to the ones without correction, implying that even if the magnitude of turbulent velocities may differ between methods, the relation between C_μ and α_M remains unaltered.

[12] The best-fit value for b is close to -0.5, which, as we will demonstrate now, leads to a simplified prediction of the turbulence production. With $b = -0.5$, $C_{\mu\ \mathrm{GR}} = a_2\alpha_M^{-0.5} = a_2(S^2k^2/\varepsilon^2)^{-0.5} = a_2\varepsilon/(Sk)$. Accordingly, $\nu_{t\ \mathrm{GR}} = C_{\mu\ \mathrm{GR}}k^2/\varepsilon = a_2k/S$, implying that $P = \nu_tS^2$ becomes

$$P_{\mathrm{GR}} = a_2\,k\,S. \tag{5}$$

With the best-fit $a_2 = 0.083 \pm 0.003$, we indeed obtain high skill (Figure 3), with $r^2 = 0.94$ and $e_{rms} = 4 \times 10^{-5}(\mathrm{m^2/s^3})$. We note that this skill was obtained although the turbulent kinetic energy and Reynolds stresses were substantially less well related, with $r^2 = 0.55$ and 0.52 for $(k, \overline{u'w'})$ and $(k, \overline{v'w'})$, respectively. Figure 3 also demonstrates that the production estimated with the stability function of *Canuto et al.* [2001] overestimated observed P_{Re} by a factor of 3. Interestingly, equation (5) is consistent with the model of *Guimet and Laurence* [2002], based on a turbulent production source term that is linear with respect to strain, applied to impinging flows for which the standard model is well known to overestimate the production of kinetic energy. However, we are not aware of other field measurements attesting this behavior in natural surf zones. Finally, equation (5) does not depend on ε and can thus be used in one-equation turbulent-viscosity models as well.

4. Conclusions

[13] Here, we used two field data sets to derive a new parameterization of the stability function C_μ (i.e., equation (4)) in two-equation turbulence-viscosity models. The parameterization is applicable to natural surf zone conditions, which are characterized by low ratios of production to dissipation ratio (here, ≈0.15) and significant vertical turbulence diffusion. Consistent with earlier work, we find C_μ to depend on the nondimensional shear frequency but our observed C_μ are substantially lower (factor 2–5) than those predicted with existing parameterizations as these assume turbulence diffusion to be negligible. Our new C_μ parameterization can also be rewritten into an expression that accurately ($r^2 = 0.94$) reproduced Reynolds-stress based observations of shear production (i.e., equation (5)). This expression does not contain the turbulence dissipation rate and is thus also applicable in one-equation turbulent-viscosity models. We anticipate our work to improve turbulence modeling in natural surf zones and to eventually lead to more reliable predictions of coastal evolution in response to severe storms.

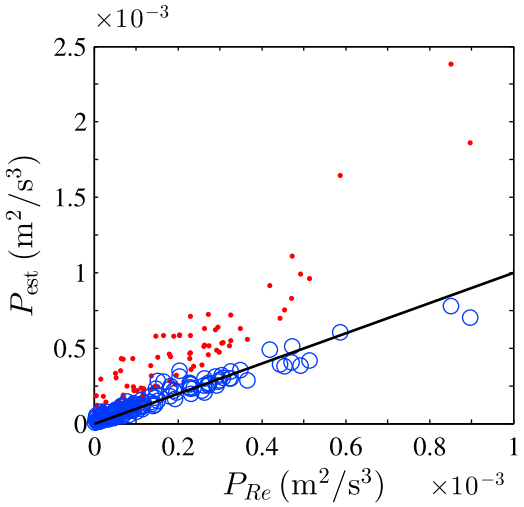

Figure 3. Turbulent production estimated with the stability function of *Canuto et al.* [2001] (P_{C01}, dots) and estimated by the formula proposed in this study (P_{GR}, circles) versus the Reynolds-stress turbulent production (P_{Re}) for Truc Vert and Ameland experiments. The solid line is the line of equality. Here, $P_{\mathrm{GR}} = 0.083\ k\ S$ with skill $r^2 = 0.94$ and $e_{rms} = 4 \times 10^{-5}$ m^2/s^3.

[14] **Acknowledgments.** The 'Truc Vert 2008' and 'Ameland 2010' field data were collected as part of the multi-institutional ECORS (SHOM-DGA) project, and a MSc research project within the Coastal Research Group at Utrecht University, respectively. We are greatly indebted to Marcel van Maarseveen and Henk Markies for the electronic and mechanic design of the rig and their excellent field support. Aline Pieterse and Anouk de Bakker are warmly acknowledged for their excellent work during 'Ameland 2010'. We also want to thank Damien Violeau and David Hurther for fruitful discussions. Funded by the Netherlands Organisation for Scientific Research NWO (Rubicon/Marie Curie Cofund Action) under project 825.10.034.

[15] The Editor thanks two anonymous reviewers for their assistance in evaluating this paper.

References

Almar, R., B. Castelle, B. G. Ruessink, N. Sénéchal, P. Bonneton, and V. Marieu (2010), Two- and three-dimensional double-sandbar system behaviour under intense wave forcing and meso-macro tidal range, *Cont. Shelf Res.*, *30*, 781–792.

Burchard, H. (2001), Simulating the wave-enhanced layer under breaking surface waves with two-equation turbulence models, *J. Phys. Oceangr.*, *31*(11), 3133–3145.

Burchard, H., and K. Bolding (2001), Comparative analysis of four second-moment turbulence closure models for the oceanic mixed layer, *J. Phys. Oceangr.*, *31*, 1943–1968.

Canuto, V. M., A. Howard, Y. Cheng, and M. S. Dubovikov (2001), Ocean turbulence. Part I: One-point closure model-momentum and heat vertical diffusivities, *J. Phys. Oceangr.*, *31*, 1413–1426.

Feddersen, F. (2010), Quality controlling surfzone acoustic doppler velocimeter, observations to estimate the turbulent dissipation rate, *J. Atmos. Oceanic Technol.*, *27*, 2039–2055.

Feddersen, F. (2012a), Observations of the surfzone turbulent dissipation rate, *J. Phys. Oceangr.*, *42*, 386–399.

Feddersen, F. (2012b), Scaling surf zone turbulence, *Geophys. Res. Lett.*, *39*, L18613, doi:10.1029/2012GL052970.

Feddersen, F., and J. H. Trowbridge (2005), The effect of wave breaking on surf-zone turbulence and alongshore currents: A modeling study, *J. Phys. Oceangr.*, *35*(11), 2187–2203.

Feddersen, F., and A. J. Williams III (2007), Direct estimation of the Reynolds stress vertical structure in the nearshore, *J. Atmos. Oceanic Technol.*, *24*, 102–116.

Gerbi, G. P., J. H. Trowbridge, E. A. Terray, A. J. Plueddemann, and T. Kukulka (2009), Observations of turbulence in the ocean surface boundary layer: Energetics and transport, *J. Phys. Oceangr.*, *39*, 1077–1096.

Grasso, F., B. Castelle, and B. G. Ruessink (2012), Turbulence dissipation under breaking waves and bores in a natural surf zone, *Cont. Shelf Res.*, *43*, 133–141.

Guimet, V., and D. Laurence (2002), A linearised turbulent production in the k-epsilon model for engineering applications, *Eng. Turbul. Modell. Exp.*, *5*, 157–166.

He, H., and D. Chen (2011), Effects of surface wave breaking on the oceanic boundary layer, *Geophys. Res. Lett.*, *38*, L07604, doi:10.1029/2011GL046665.

Hurther, D., and U. Lemmin (2001), A correction method for turbulence measurements with a 3D Acoustic Doppler Velocity Profiler, *J. Atmos. Oceanic Technol.*, *18*, 446–458.

MacMahan, J. H. M., et al. (2010), Mean Lagrangian flow behavior on an open coast rip-channeled beach: A new perspective, *Mar. Geol.*, *268*, 1–15.

Mellor, G. L., and T. Yamada (1982), Development of a turbulence closure model for geophysical fluid problems, *Rev. Geophys.*, *20*(4), 851–875.

Melville, W. K., F. Veron, and C. White (2002), The velocity field under breaking waves: coherent structures and turbulence, *J. Fluid Mech.*, *454*, 203–233.

Pope, S. B. (1975), A more general effective-viscosity hypothesis, *J. Fluid Mech.*, *72*, 331–340.

Pope, S. B. (2000), *Turbulent Flows*, 1st ed., Cambridge Univ. Press, Cambridge, U. K.

Rodi, W. (1976), A new algebraic relation for calculating the Reynolds stresses, *Z. Angew. Math. Mech.*, *56*, 219–221.

Rodi, W. (1987), Examples of calculation methods for flow and mixing in stratified fluids, *J. Geophys. Res.*, *92*(C5), 5305–5328.

Ruessink, B. G. (1998), Bound and free infragravity waves in the nearshore zone under breaking and nonbreaking conditions, *J. Geophys. Res.*, *103*(C6), 12,795–12,805.

Ruessink, B. G. (2010), Observations of turbulence within a natural surf zone, *J. Phys. Oceangr.*, *40*, 2696–2712.

Ruessink, B. G., and Y. Kuriyama (2008), Numerical predictability experiments of cross-shore sandbar migration, *Geophys. Res. Lett.*, *35*, L01603, doi:10.1029/2007GL032530.

Ruessink, B. G., M. Boers, P. F. C. van Geer, A. T. M. de Bakker, A. Pieterse, F. Grasso, and R. C. de Winter (2012), Towards a process-based model to predict dune erosion along the Dutch Wadden coast, *Neth. J. Geosci.*, *91*(3), 357–372.

Scott, C. P., D. T. Cox, T. B. Maddox, and J. W. Long (2005), Large-scale laboratory observations of turbulence on a fixed barred beach, *Meas. Sci. Technol.*, *16*, 1903–1912.

Scott, N. V., T. J. Hsu, and D. T. Cox (2009), Steep wave, turbulence, and sediment concentration statistics beneath a breaking wave field and their implications for sediment transport, *Cont. Shelf Res.*, *29*, 2303–2317.

Sénéchal, N., et al. (2011), The ECORS-Truc Vert'08 nearshore field experiment: Presentation of a three-dimensional morphologic system in a macro-tidal environment during consecutive extreme storm conditions, *Ocean Dyn.*, *61*, 2073–2098, doi:10.1007/s10236-011-0472-x.

Svendsen, I. A. (1987), Analysis of surf zone turbulence, *J. Geophys. Res.*, *92*(C5), 5115–5124.

Taulbee, D. B. (1992), An improved algebraic Reynolds stress model and corresponding nonlinear stress model, *Phys. Fluids A*, *4*, 2555–2561.

Tennekes, H., and J. L. Lumley (1972), *A First Course in Turbulence*, 1st ed., MIT Press, Cambridge, Mass.

Ting, F. C. K., and J. T. Kirby (1996), Dynamics of surf-zone turbulence in a spilling breaker, *Coast. Eng.*, *27*, 131–160.

Trowbridge, J., and S. Elgar (2001), Turbulence measurements in the surf zone, *J. Phys. Oceangr.*, *31*, 2403–2417.

Umlauf, L., and H. Burchard (2005), Second-order turbulence closure models for geophysical boundary layers. A review of recent work, *Cont. Shelf Res.*, *25*, 795–827.

Violeau, D. (2009), Explicit algebraic Reynolds stresses and scalar fluxes for density-stratified shear flows, *Phys. Fluids*, *21*, 035103, doi:10.1063/1.3081552.

Wallin, S., and A. V. Johansson (2000), An explicit algebraic Reynolds stress model for incompressible and compressible turbulent flows, *J. Fluid Mech.*, *403*, 89–132.